Murine prolylcarboxypeptidase depletion induces vascular dysfunction with hypertension and faster arterial thrombosis

Gregory N. Adams,[1,2] Gretchen A. LaRusch,[1] Evi Stavrou,[1] Yihua Zhou,[1] Marvin T. Nieman,[1,3] Gretta H. Jacobs,[2] Yingjie Cui,[4] Yuan Lu,[4] Mukesh K. Jain,[4] Fakhri Mahdi,[5] Zia Shariat-Madar,[6] Yoshio Okada,[7] Louis G. D'Alecy,[8] and Alvin H. Schmaier[1,2]

[1]Department of Medicine, Hematology and Oncology Division, [2]Department of Pathology, [3]Department of Pharmacology, and [4]University Hospitals Harrington-McLaughlin Heart & Vascular Institute and Case Cardiovascular Research Institute, Case Western Reserve University, Cleveland OH; Departments of [5]Pharmacognosy and [6]Pharmacology, University of Mississippi, Oxford, MS; [7]Department of Medicinal Chemistry, Kobe Gakuin University, Kobe, Japan; and [8]Department of Physiology, University of Michigan, Ann Arbor, MI

Prolylcarboxypeptidase (PRCP) activates prekallikrein to plasma kallikrein, leading to bradykinin liberation, and degrades angiotensin II. We now identify PRCP as a regulator of blood vessel homeostasis. β-Galactosidase staining in PRCP[gt/gt] mice reveals expression in kidney and vasculature. Invasive telemetric monitorings show that PRCP[gt/gt] mice have significantly elevated blood pressure. PRCP[gt/gt] mice demonstrate shorter carotid artery occlusion times in 2 models, and their plasmas have increased thrombin generation times. Pharmacologic inhibition of
PRCP with Z-Pro-Prolinal or plasma kallikrein with soybean trypsin inhibitor, Pro-Phe-Arg-chloromethylketone or PKSI 527 also shortens carotid artery occlusion times. Aortic and renal tissues have uncoupled eNOS and increased reactive oxygen species (ROS) in PRCP[gt/gt] mice as detected by dihydroethidium or Amplex Red fluorescence or lucigenin luminescence. The importance of ROS is evidenced by the fact that treatment of PRCP[gt/gt] mice with antioxidants (mito-TEMPO, apocynin, Tempol) abrogates the hypertensive, prothrombotic phenotype.
Mechanistically, our studies reveal that PRCP[gt/gt] aortas express reduced levels of Kruppel-like factors 2 and 4, thrombomodulin, and eNOS mRNA, suggesting endothelial cell dysfunction. Further, PRCP siRNA treatment of endothelial cells shows increased ROS and uncoupled eNOS and decreased protein C activation because of thrombomodulin inactivation. Collectively, our studies identify PRCP as a novel regulator of vascular ROS and homeostasis. (*Blood*. 2011;117(14): 3929-3937)

Introduction

Prolylcarboxypeptidase (PRCP; lysosomal carboxypeptidase) is a cell surface enzyme in the S28 class of serine proteases. PRCP dimerizes and has a unique protease structure with closest identity to dipeptidyl peptidase 7 with a novel helical structural domain (SKS domain) that caps the active site of the catalytic Asp-His-Ser triad.[1,2] The protein was first isolated from swine kidney lysosomal fractions and identified as a bradykinin and angiotensin II carboxypeptidase.[3] PRCP is found on the surface of endothelial cells where it is a high-affinity activator that converts prekallikrein bound to high molecular weight kininogen to the serine protease plasma kallikrein.[4,5] PRCP proteolyzes penultimate C-terminal prolines, except for bradykinin (RPPGFPFR) where it cleaves between the Pro and Phe.[6] The molecular affinity of PRCP for Pro-X bonds is demonstrated by its crystal structure with the identification of hydrophobic residues near the substrate proline at the active site.[1,2] PRCP is up-regulated during the angiogenic processes of vascular development.[7]

The exact physiologic role for PRCP is not completely known. A PRCP polymorphism (E112D) is linked to hypertension and preeclampsia.[8,9] Further, PRCP is up-regulated in the kidney in a rat hypertension model.[10] PRCP is linked to metabolic syndrome in humans.[11] PRCP also degrades α-melanocyte stimulating hormone (α-MSH$_{1-13}$) to its inactive α-MSH$_{1-12}$ form by cleaving its

C-terminal Val.[12] α-MSH$_{1-13}$ stimulates an anorexigenic response. PRCP gene-trap mice are lean because of reduced hypothalamic α-MSH$_{1-13}$ degradation.[12] Because PRCP activates prekallikrein and degrades angiotensin II, we determined whether PRCP genetrap mice have a cardiovascular phenotype. PRCP gene-trap hypomorphs demonstrate constitutively higher blood pressure and shorter arterial vessel closure times. PRCP depletion in tissues and cells is associated with increased uncoupled eNOS and reactive oxygen species (ROS). In PRCP-depleted mice and cultured cells, increased ROS is associated with endothelial cell dysfunction and loss of anticoagulant properties.

Methods

Materials

The chromogenic substrates H-D-Pro-Phe-Arg-pNA·2HCl (S-2302) and Glu-Pro-Arg-pNA·2HCl (S-2366) were purchased from DiaPharma, and plasma prekallikrein activator was purchased from Enzyme Research Laboratories. The fluorescent thrombin-specific substrate Z-Gly-Gly-Arg-AMC·2HCl was purchased from Bachem. Innovin PT reagent as a source of recombinant, human tissue factor, and APTT reagent were obtained from Siemens. Rossix phospholipid mixture was purchased from DiaPharma.

The polyclonal goat anti–mouse-PRCP antibody (anti-TND20) was reared with a peptide from the mouse PRCP amino acid sequence TNDFRKS-GPYCSESIRKSWN at Q.C.B. Custom Antibody Service. Human coagulation factors XIIa, XIa, and plasma kallikrein were purchased from Enzyme Research Laboratories. Lactic dehydrogenase (LDH) assay was obtained from Sigma-Aldrich. PKSI-527 was from Dr Yoshio Okada, Kobe Gakuin University, Kobe, Japan.[13] Mouse anti–human antibody to thrombomodulin was obtained from Santa Cruz Biotechnology (sc-13164).

Preparation of the murine PRCP hypomorph

ES cells KST302 prepared by gene trap were obtained from Bay Genomics as previously reported.[12,14] The CD4-β-geo-SV40 targeting vector to membrane-expressed proteins was injected into 129svj ES cells and incorporated into intron 4 of mouse PRCP.[14] Mice in 129svj background, made from the Prcp interrupted ES cells (KST302), were then back-crossed 10 generations into C57BL/6 mice.[12] Tail DNA was used to genotype mice possessing the β-geo transgene with the following primer sequences: forward, 5′-TTACAACGTCGTGACTGGGA-3′; reverse, 5′-TTAC-GTTGGTGTAGATGGGC-3′. Mice with the gene insertion replace Prcp with LacZ.[14]

Murine blood pressure measurements

Blood pressure in the mice was measured by telemetry as previously described using C-10 transmitters from DSI.[15] After implantation of the sensing catheter and transmitter, the mice were allowed to recover for 7 days until a circadian rhythm was observed. Data were collected with Dataquest ART software Version 4.1 continuously for 4 days and analyzed as a running average every hour. MitoTEMPO (Enzo Life Sciences) was delivered to mice by osmotic pump at a dose of 0.7 mg/kg per day for 2 weeks before blood pressure measurement. In the analysis of the continuous blood pressure data, the values on the graph represent mean arterial pressure (MAP) for the following hour. Differences among/between groups were determined by comparing the 8-hour periods in the night or day cycle after the initial 4-hour transition period from day to night or night to day, respectively, was excluded. All animal experiments were approved by the Case Western Reserve University Institutional Animal Care and Use Committee.

Arterial thrombosis assays

The Rose-Bengal carotid artery thrombosis assay was performed as described previously with mice anesthetized with 40 mg/kg sodium pento-barbital intraperitoneally.[16] The ferric chloride-induced carotid artery damage was performed with a 1 mm × 1 mm filter paper soaked in 4% $FeCl_3$ and placed on the carotid artery for one minute. In the arterial thrombosis studies, tempol (Enzo Life Sciences) was crushed and placed into a soft dough diet (Transgenic Dough Diet, Bio-Serv) at a dose of 10 mg of drug/gram of food and made fresh daily for 7 days. In the Amplex Red studies, 1mM tempol was dissolved in drinking water, and the mice were treated for 3 weeks before study. In other experiments, apocynin (Sigma-Aldrich) was dissolved at 14mM in drinking water containing a sweetener (Equal), and the mice were treated for 7 days. Arterial thrombosis studies were performed on C57BL/6 or 129svj wild-type (WT) mice after intraperitoneal injection with various pharmacologic inhibitors delivered at the following concentrations: Pro-Phe-Arg-chloromethylketone (PFRCK; Bachem), 10 mg/kg; soybean trypsin inhibitor (SBTI; Calbio-chem), 30 mg/kg; the plasma kallikrein inhibitor PKSI-527,[14] 50 mg/kg; or Z-Pro-Prolinal (ZPP; Bachem, 10 mg/kg).

Determination of uncoupled eNOS

Uncoupled to coupled eNOS ratios were obtained from renal tissue or cultured human umbilical vein endothelial cells (HUVECs) digested in cold RIPA buffer containing protease inhibitors and 5% β-mercaptoethanol without boiling and separated on 5% sodium dodecyl sulfate-polyacryl-amide gel electrophoresis maintained at 4°C.[17] The protein on the gels was then transferred for 3 hours at 4°C to nitrocellulose membranes, and protein detected with an eNOS antibody (sc-654, Santa Cruz Biotechnology) at

0.4 μg/mL. Coupled (top) and uncoupled (bottom) band density ratios were determined using densitometry (Scion Image).[18] Ratios were standardized to the average WT ratio values of RIPA-buffer homogenized samples.

Assays for ROS

Dihydroethidium (DHE) fluorescent analysis was performed on frozen tissue sections (4 μm kidney, 7 μm aorta) incubated with the agent (1 μm for kidney, 2 μm for aorta) for 5 minutes, and washed with phosphate-buffered saline (PBS).[19] Confocal images were analyzed by morphometric analysis of pixels per nucleus using MetaMorph software Version 7 (Molecular Devices). The color threshold was set the same for each image, and the red pixel density was obtained by dividing the total pixel density value by the number of nuclei in the smooth muscle and endothelial layers or renal cortex. Lucigenin measurements were obtained by placing 3-mm pieces of aorta into 96-well plate wells containing 50μM lucigenin (Sigma-Aldrich) in warm Krebs-N-2-hydroxyethylpiperazine-N′-2-ethane-sulfonic acid buffer (99mM NaCl, 4.7mM KCl, 1.2mM $MgSO_4$, 1.9mM $CaCl_2$, 25mM $NaHCO_3$, 11.1 glucose, 20mM N-2-hydroxyethylpiperazine-N′-2-ethanesulfonic acid, pH 7.4).[20] Aortas were collected and cleaned in cold Krebs-N-2-hydroxyethylpiperazine-N′-2-ethanesulfonic acid buffer and placed at 37°C for 30 minutes. Before obtaining luminescent values for each sample, background luminescent values were obtained from each well (NOVOstar; BMG Labtech). Values were standardized to supernatants of 1% Triton solubilized aorta by LDH determination. Lucigenin measure-ments of renal samples were normalized by milligram of protein studied. Renal hydrogen peroxide was measured using Amplex Red (100μM) with 10 U/mL horseradish peroxidase, according to the manufacturer's sugges-tions (Invitrogen).[21] Fluorescent readings were obtained from mouse kidneys after 1-hour incubation at 37°C, and values were normalized to dried tissue weight.

Cell culture experiments

HUVECs were purchased from AllCells and grown on gelatin-coated plates in CSC media (Cells Systems). Cells were grown to near-confluence in 6-well plates and transfected with Lipofectamine 2000 reagent (Invitrogen) in OPTI-MEM media (Invitrogen) overnight. Sequences of siRNA (Ambion) were as follows (5′ to 3′): human-*PRCP*: sense, GGCUGAU-UUUGCAGAGUUAtt; antisense, UAACUCUGCAAAAUCAGCCag; negative control: sense, UAACGACGCGACGACGUAAtt; and antisense, UUACGUCGUCGCGUCGUUAtt. Cells were then washed with PBS and placed in CSC medium. DHE staining (10μM) was performed in PBS for 30 minutes at 37°C. After washing, images were obtained with a Nikon Eclipse TE200 microscope and a Nikon 10×/0.25 objective lens. The images were analyzed with Metamorph software Version 7 and values obtained by calculating pixel density per nucleus. Protein C activation studies were measured on siRNA-treated HUVECs on 96-well plates. The cells were washed with N-2-hydroxyethylpiperazine-N′-2-ethanesulfonic acid carbonate buffer (137mM NaCl, 3mM KCl, 12mM $CaHCO_3$, 5.5mM dextrose, 0.1% gelatin, 1mM $CaCl_2$, 1mM $MgCl_2$, pH 7.1) and incubated for 1 hour at 37°C with 0.5nM thrombin (Haematologic Technologies) and 0.5nM protein C (Enzyme Research). The reaction was stopped by 10 U/mL hirudin (Sigma-Aldrich). Hydrolysis of the chromogenic substrate S-2366 (0.3mM; DiaPharma) was analyzed by calculating the initial slope of 405-nm absorbance.

Mouse embryonic fibroblast (MEF) cell cultures were prepared from E13 embryos of WT and $PRCP^{gt/gt}$ mice.[22] The embryos were dissected from the womb under sterile conditions and washed with PBS. Embryo heads and red organs were removed, and the remaining tissue was minced and digested with 0.25% trypsin for 20 minutes at 37°C. Cell suspensions were plated in Dulbecco modified Eagle medium with 10% fetal bovine serum and penicillin/streptomycin.[22] MEFs were immortalized with Large T in LNCX2 in lentivirus generously supplied by Mark Jackson, Case Western Reserve University.

Statistical analyses

One-way analysis of variance was used to determine the differences among groups. Unless stated otherwise in text, all groups indicated differences.
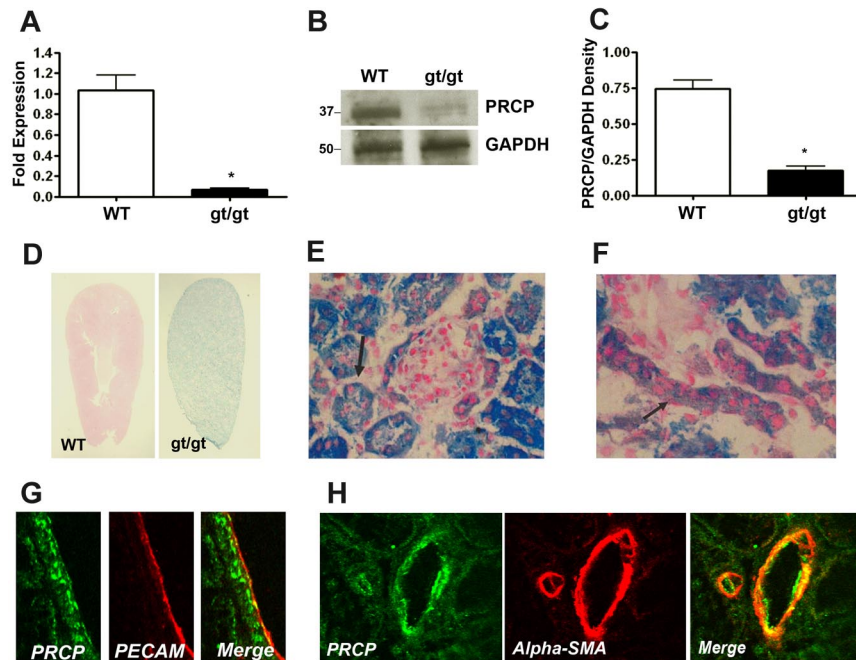
Figure 1. Characterization of the PRCP hypomorph (PRCP$^{gt/gt}$) mouse. (A) Total renal mRNA was reverse-transcribed to cDNA from C57BL/6 (WT) and PRCP$^{gt/gt}$ (gt/gt) mice, and quantitative PCR was performed. Data represent mean ± SEM of PCR studies from 3 mice in each group. (B) PRCP antigen level was detected by immunoblot with a goat antimouse-PRCP antibody (anti-TND-20) on 100 μg of renal lysate from WT or PRCP$^{gt/gt}$ mice. Anti-GAPDH antibody was used as a loading control. (C) Comparative antigen levels from panel B were quantified with densitometry. The bar graph is the mean ± SEM ratio of PRCP/GAPDH antigen in 4 WT or PRCP$^{gt/gt}$ renal lysates. (D) Longitudinal sections of X-Gal–stained whole mouse kidney from WT and PRCP$^{gt/gt}$ (gt/gt) mice. Kidney sections were stained for LacZ with X-Gal to determine the presence of the CD4TM-β-geo transgene in place of the Prcp gene. Blue LacZ staining in the PRCP$^{gt/gt}$ indicates where endogenous PRCP would be expressed in these tissues from WT mice. The photographs were taken on a Nikon SMZ-U dissecting microscope at 2× magnification. (E) Cross section of X-Gal–stained renal cortex from a PRCP$^{gt/gt}$ mouse showing a Bowman capsule of a glomerulus with LacZ protein and variably darkly stained tubules. The black arrow points to a darkly stained tubule. (F) Longitudinal vessel sections from renal cortex from a PRCP$^{gt/gt}$ mouse showing staining for the LacZ protein, which replaces PRCP.[14] The figure is at 40× magnification. Black arrow points to vascular PRCP as indicated by the presence of LacZ. (E-F) Photographed on an Olympus BH-2 microscope aperture 0.70 160/0.17 at 40×. Arterial PRCP was colocalized with the endothelial cell marker PECAM (CD31; G) and the vascular smooth muscle cell marker α-smooth muscle actin (α-SMA; H). (G-H) Photographed on a Zeiss LSM510 confocal microscope aperture 40×/1.3 oil immersion. *$P < .05$.

Unpaired t test was used to determine differences between groups. Data are compared as mean ± SD in text and graphed as mean ± SEM using GraphPad Prism software Version 4. Statistical significance is defined as a $P < .05$.

Histologic, mRNA, and immunoblot studies and in vitro assay methods are in supplemental Data (available on the *Blood* Web site; see the Supplemental Materials link at the top of the online article).

Results

Characterization of PRCP$^{gt/gt}$ mice

PRCP gene-trap mice (PRCP$^{gt/gt}$) were produced by random transgene incorporation into intron 4, allowing for interruption of mRNA production.[12,14] In kidney, PRCP$^{gt/gt}$ mice express 6.5% ± 2.3% Prcp mRNA (mean ± SD) compared with WT (Figure 1A). PRCP$^{gt/gt}$ mice have 23% PRCP antigen (Figure 1B-C). PRCP$^{gt/gt}$ mice are not true "knockout" mice, but rather, hypomorphs. PRCP$^{gt/gt}$ mice express LacZ protein in place of PRCP. X-Gal staining, which demonstrated endogenous PRCP expression disrupted in PRCP$^{gt/gt}$ tissues, showed that the kidney was the major site for expression (Figure 1D). At low magnification, X-Gal staining of longitudinally sectioned kidneys demonstrated a gross blue-green appearance, indicating that normal kidney has a high PRCP concentration (Figure 1D). Microscopic analysis of renal cortex showed dark X-gal staining in some tubules and lighter staining in others (Figure 1E). Bowman capsules adjacent to the darkly stained tubules were thickened with a heavy X-Gal stain

(Figure 1E). X-Gal staining was also observed in renal vessels (Figure 1F). Renal tubule PRCP colocalized with the glycoprotein Lotus lectin, indicating that the darkly stained X-Gal structures were proximal tubules (supplemental Figure 1A). Lotus lectin and immunoperoxidase staining showed that proximal tubule PRCP was localized on the basal side of the cells (supplemental Figure 1A-B). Renal artery PRCP colocalized with both PECAM antigen on endothelium (Figure 1G) and α-smooth muscle actin in vascular smooth muscle (Figure 1H). Smaller amounts of X-Gal staining were seen in brain, small bowel, and testes (supplemental Figure 1C-E).

Hypertension phenotype of PRCP$^{gt/gt}$ mice

On review of the hematoxylin and eosin renal histology, we observed that some glomerular Bowman capsules of 6-month-old PRCP$^{gt/gt}$ mice show "tubulization," a histologic marker for hypertension (Figure 2A).[23,24] Continuous carotid artery blood pressure monitoring was performed by telemetry. The stable MAP during 8 hours of the night cycle (10 PM to 6 AM) was significantly higher in the PRCP$^{gt/gt}$ mice (122 ± 6 mm Hg) compared with WT mice (113 ± 6 mm Hg; $P = .01$; Figure 2B-C). MAP during the 8 hours of the day from 10 AM to 6 PM also was significantly higher in PRCP$^{gt/gt}$ mice (114 ± 8 mm Hg) compared with WT (106 ± 8 mm Hg; $P < .044$) on differences between groups, but not on a one-way analysis of variance among the 3 groups. When PRCP$^{gt/gt}$ mice were treated with the mitochondrial-specific superoxide scavenger mitoTEMPO, the MAP of the treated PRCP$^{gt/gt}$
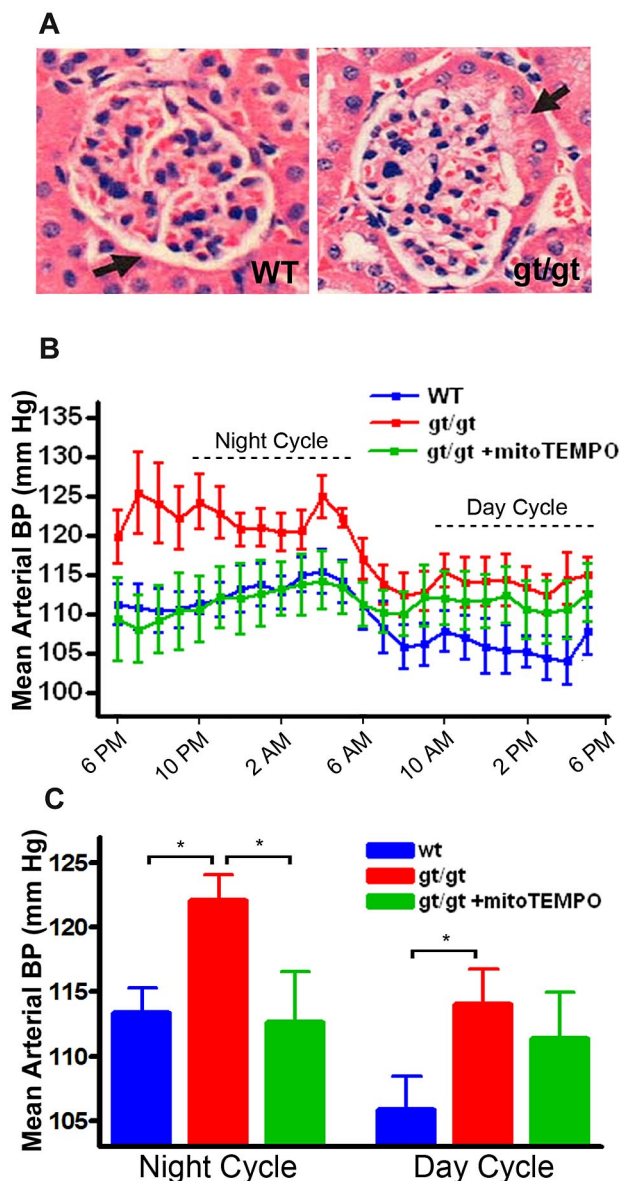
Figure 2. Characterization of the blood pressure of PRCP[gt/gt] mice. (A) Hematoxylin and eosin staining of 6-month-old mouse kidney are shown from WT and PRCP[gt/gt] mice. A thickened Bowman capsule (tubulization) is noted in the PRCP[gt/gt] mice (compare thickness of Bowman capsule in WT vs gt/gt sections, black arrow). The images were photographed on an Olympus BH-2 microscope aperture 0.70 160/0.17 at 40×. (B) Carotid artery blood pressure measurement by a sensor for telemetry was performed on WT and PRCP[gt/gt] mice (gt/gt; "Murine blood pressure measurements"). Hourly data were compiled from 4 days of measurement. Data are mean ± SEM of monitoring 9 WT, 8 PRCP[gt/gt], and 3 mitoTEMPO-treated PRCP[gt/gt] (gt/gt+mitoTEMPO) mice. The dotted lines indicate an 8-hour period of the night or day cycle, respectively, used to analyze differences between groups. (C) Hourly data expressed in panel B are presented as an 8-hour period of the night or day cycle, respectively. One-way analysis of variance was used to determine differences among groups. *P < .05.

mice during the night cycle (113 ± 7 mm Hg) was significantly reduced compared with untreated gene-trap mice (122 ± 6 mm Hg; P = .04).[25] These data indicated that PRCP[gt/gt] mice have antioxidant-responsive hypertension.

Expression of ROS in PRCP[gt/gt]

Because the PRCP[gt/gt] mice have antioxidant responsive hypertension, we sought evidence for increased tissue ROS.[26] The superox-

ide ($O_2^{·−}$) fluorescent probe DHE showed increased fluorescent intensity in PRCP[gt/gt] aorta (P = .01) and kidney (P = .04; Figure 3A-B). PRCP[gt/gt] mice had 3.2-fold and 2.8-fold brighter fluorescence in aortic and renal sections, respectively (Figure 3A-B). PRCP[gt/gt] mice also demonstrated a 1.6-fold increase (P = .04) in approximately 3-mm-long aortic pieces (arbitrary luminescent units [ALU]/LDH units) and a 1.7-fold increase (P = .02) in kidney lysates (ALU/mg-protein) in PRCP[gt/gt] tissue vs control using the chemiluminescent superoxide probe lucigenin (Figure 3C-D). Renal tissue from PRCP[gt/gt] additionally showed a 2.4-fold increase (P = .04) in Amplex Red fluorescence, a measure of hydrogen peroxide (H_2O_2), compared with WT mice (Figure 3E). Last, we determined that there was a higher ratio of uncoupled eNOS to coupled eNOS in renal tissue from PRCP[gt/gt] mice compared with WT mice (P = .02; Figure 3F). Uncoupled eNOS additionally propagates superoxide production. These combined data indicated that renal and vascular tissue in the PRCP[gt/gt] mice is injured.

### Arterial occlusion times in PRCP[gt/gt] mice

Because aortas were found to express increased ROS, PRCP[gt/gt] mice were examined for changes in arterial occlusion times. On the Rose Bengal assay for induced carotid artery thrombosis, PRCP[gt/gt] mice had a faster time to carotid artery occlusion on vessel insult (24 ± 3 minutes) than their C57BL/6 controls (52 ± 8 minutes; P < .01; Figure 4A). Using 4% ferric chloride to induce carotid artery thrombosis, no WT mice occluded by 60 minutes, whereas all PRCP[gt/gt] occluded in 21 ± 8 minutes (Figure 4A). Additional investigations determined whether pharmacologic inhibition of PRCP or its protein product, plasma kallikrein, also produced a shortened arterial occlusion time. In WT C57BL/6 mice, the prolyloligoprotease inhibitor Z-Pro-Prolinal (ZPP; 10 mg/kg intraperitoneally) shortened the time to arterial occlusion on the Rose Bengal assay from 48 ± 5 minutes to 24 ± 5 minutes (P < .01; Figure 4B). Likewise, when the WT C57BL/6 mice were treated with SBTI (30 mg/kg intraperitoneally), PFRCK (10 mg/kg intraperitoneally), or the specific plasma kallikrein inhibitor, PKSI-527 (50 mg/kg intraperitoneally), the time to arterial thrombosis shortened to 28 ± 4 minutes (P < .01), 28 ± 7 minutes (P < .01), and 15 ± 4 minutes (P < .01), respectively (Figure 4B). Pharmacologic inhibition of PRCP and plasma kallikrein also shortened occlusion times in 129svj WT mice (22 ± 3 minutes; supplemental Figure 2). When these mice were treated with ZPP, SBTI, PFRCK, or PKSI-527, the carotid artery occlusion times on the Rose Bengal assay significantly shortened to 11 ± 1 minute (P < .01), 12 ± 4 minutes (P < .01), 10 ± 1 minute (P < .01), and 13 ± 2 minutes (P < .01), respectively (supplemental Figure 2).

PFRCK and SBTI are nonspecific serine protease inhibitors. Investigations determined their relative inhibition of plasma kallikrein versus factors XIIa or XIa, respectively. PFRCK is a 23-fold more potent inhibitor of 2nM plasma kallikrein than 2nM factor XIIa (50% inhibitory concentration [IC_{50}] = 0.072μM vs 1.67μM, respectively; Figure 4C). Likewise, SBTI is a 61-fold better inhibitor of 5nM plasma kallikrein than 5nM factor XIa (IC_{50} = 5.7nM vs 350nM, respectively; Figure 4D). These combined investigations indicated that pharmacologic inhibition of PRCP or plasma kallikrein produced a prothrombotic phenotype.

Plasma phenotype of PRCP[gt/gt] mice

The etiology of the prothrombotic phenotype of PRCP[gt/gt] mice was sought. PRCP[gt/gt] mice had significantly increased plasma PK

Figure 3. Measurement of tissue ROS in PRCP^{gt/gt} mice. (A-B) Studies on the expression of fluorescence in aorta (A) and kidney (B). Frozen aortas and kidneys from WT and PRCP^{gt/gt} (gt/gt) were stained with DHE. (A-B) Photographed on a Zeiss LSM510 confocal microscope aperture 40×/1.3 oil immersion. The relative DHE fluorescence was measured by morphometric analysis on 40× microscopic images using MetaMorph (Molecular Devices). Data are expressed as the number of fluorescent pixels per nuclei. Data are mean ± SEM of ≥ 9 samples on aorta and ≥ 4 samples on kidney. (C) Superoxide levels ($O_2\cdot^-$) were measured from freshly harvested mouse aortas using the chemiluminescent probe lucigenin. Data are mean ± SEM ratio of ALU per LDH units from WT or PRCP^{gt/gt} aortic pieces. (D) Superoxide levels ($O_2\cdot^-$) were determined from N-2-hydroxyethylpiperazine-N′-2-ethanesulfonic acid buffer solubilized mouse kidneys using the chemiluminescent probe lucigenin. Data are mean ± SEM ratio of arbitrary lucigenin fluorescent units (ALU) per milligram of renal tissue from WT or PRCP^{gt/gt}. (E) Hydrogen peroxide levels (H_2O_2) were determined from harvested mouse kidneys using Amplex Red. Data are mean ± SEM ratio of AFU per milligram of dried renal tissue from WT or PRCP^{gt/gt}. (F) An immunoblot for eNOS was performed on renal lysates from WT and PRCP^{gt/gt}. The normalized relative ratio of renal uncoupled/coupled eNOS in lysates from 10 mice from WT and PRCP^{gt/gt} was compared by analysis of band intensity using densitometer scanning. Immunoblot of high molecular weight kininogen was used as a loading control. *$P < .05$.
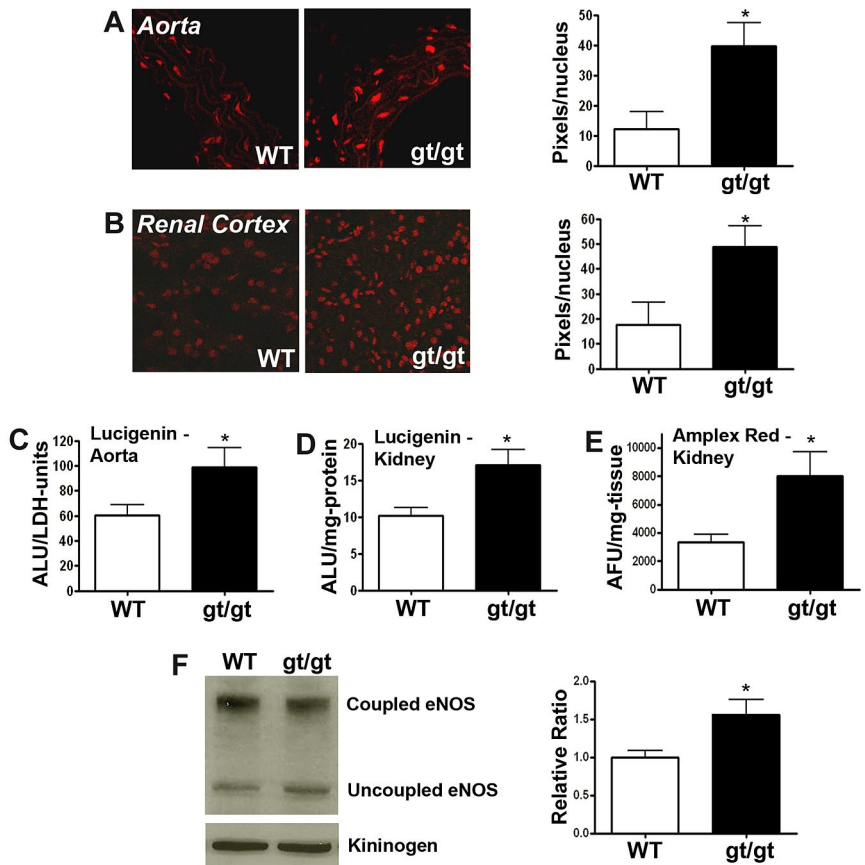
compared with WT (110% ± 10% vs 94% ± 11%; Table 1). Their plasma factor XII values (69% ± 38%) were significantly reduced compared with WT mice (114% ± 49%). Alternatively, plasma bradykinin values in the PRCP^{gt/gt} mice (0.30 ± 0.20 ng/mL) were not different from WT (0.23 ± 0.13 ng/mL). Similarly, plasma angiotensin II values were unchanged in PRCP^{gt/gt} mice compared

with WT (72 ± 41 pg/mL vs 86 ± 63 pg/mL, respectively). However, PRCP^{gt/gt} mice were found to have increased plasma thrombin generation (Table 1). When thrombin generation times were performed on contact activation-induced plasma from the PRCP^{gt/gt} versus its control, peak thrombin generation time (152 ± 9 arbitrary fluorescent units vs 131 ± 9 arbitrary fluorescent units) and
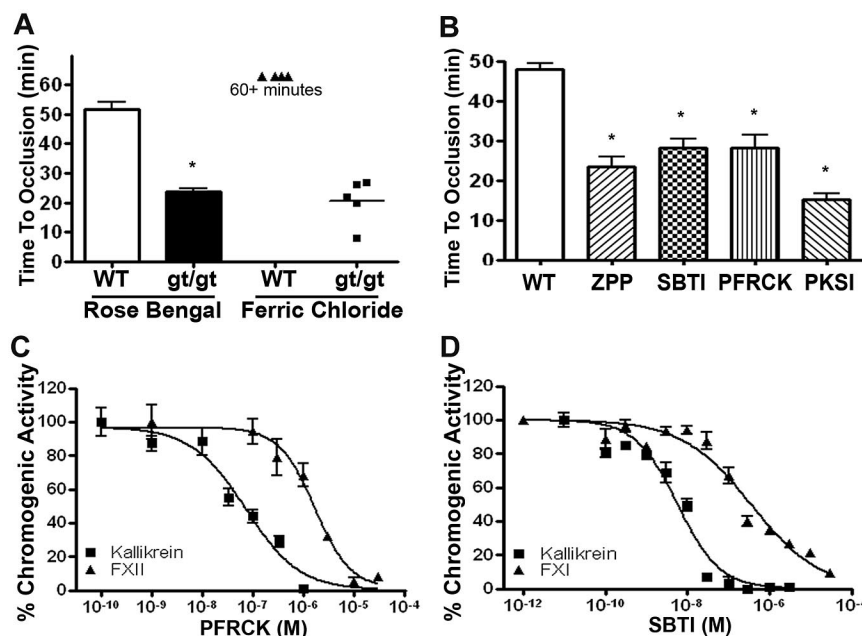

Figure 4. The influence of PRCP on arterial thrombosis risk. (A) Control C57BL/6 WT and PRCP^{gt/gt} (gt/gt) mice were subjected to the Rose-Bengal and ferric chloride carotid artery thrombosis occlusion models. Data are expressed as the time to complete arterial occlusion. A 1-way analysis of variance was used to determine differences among groups. Data represent the mean ± SEM of 10 WT and 12 PRCP^{gt/gt} mice for the Rose Bengal assay and 4 WT and 5 PRCP^{gt/gt} mice for the ferric chloride assay. (B) The time to carotid artery occlusion on the Rose Bengal assay was determined in C57BL/6 mice that were untreated (WT, open bar graph, n = 13) or treated with the inhibitor to the PRCP, ZPP (n = 4), or plasma kallikrein inhibitors SBTI (n = 4), PFRCK (n = 5), or PKSI 527 (PKSI; n = 6). Data represent the mean ± SEM of 4 to 13 animals in each group. (C) Determination of the IC₅₀ of PFRCK on 2nM plasma kallikrein or factor XIIa. Inhibition studies were performed as indicated in supplemental Methods. Data represent the mean ± SEM of 3 reactions. (D) Determination of the IC₅₀ of SBTI on 5nM plasma kallikrein or factor XIa. Inhibition studies were performed as indicated in supplemental Methods. Data represent the mean ± SEM of 3 reactions. *$P < .05$.

3934 ADAMS et al

Table 1. Characteristics of plasma proteins, peptides, and function in PRCP$^{gt/gt}$ mice

Assay	Wild-type	PRCP$^{gt/gt}$	P
Prekallikrein, % activity	94 ± 11	110 ± 11	.01
Factor XII, % activity	114 ± 49	69 ± 38	.03
Bradykinin, ng/mL	0.23 ± 0.13	0.30 ± 0.2	.24
Angiotensin, pg/mL	72 ± 41	86 ± 63	.84
Contact TGT peak, AFU	131 ± 9	152 ± 9	.02
Contact TGT AUC, AFU	18 659 ± 1255	22 608 ± 49	< .01
TF TGT peak, AFU	78 ± 5	87 ± 5	.06
TF TGT AUC, AFU	25 410 ± 1527	28 056 ± 1860	.07

Values are mean ± SD.

Contact indicates contact activation-induced thrombin generation time; TGT, thrombin generation time; AUC, area under the curve; AFU, arbitrary fluorescent units; and TF, tissue factor.

area under the curve thrombin generation time (22 608 ± 49 arbitrary fluorescent units vs 18 659 ± 1255 arbitrary fluorescent units) were significantly increased ($P = .02$ and $P < .01$, respectively). Peak and area under the curve tissue factor-induced thrombin generation time tended toward but were not significantly increased in PRCP$^{gt/gt}$ mice (Table 1). These data suggested that there was a small but significant tendency toward increased thrombin generation in the PRCP$^{gt/gt}$ mice.

Influence of ROS reduction on thrombosis

We next asked whether increased vascular ROS contributed to the shorter thrombosis times in PRCP$^{gt/gt}$ mice. When these mice were treated orally for 7 days with the antioxidant apocynin, the time to arterial thrombosis on the Rose Bengal carotid artery thrombosis assay was significantly lengthened from 36 ± 5 minutes in untreated PRCP$^{gt/gt}$ mice to 58 ± 20 minutes in treated animals ($P = .01$), a value not significantly different from WT mice ($P = .67$; Figure 5A). Apocynin treatment did not significantly alter the time to arterial thrombosis in treated WT mice ($P = .45$; Figure 5A). Similarly, when PRCP$^{gt/gt}$ mice were treated with the superoxide scavenger tempol, the time to arterial thrombosis significantly lengthened from 31 ± 3 minutes in untreated mice to 49 ± 7 minutes in

the treated PRCP$^{gt/gt}$ mice ($P < .01$; Figure 5B). Tempol treatment also had no effect on the time to thrombosis on WT mice. Tempol administration significantly decreased renal tissue ROS (H$_2$O$_2$) as measured by Amplex Red fluorescence ($P < .01$; Figure 5C). Because ROS is associated with vascular injury, we determined whether genes associated with vascular function were altered in PRCP$^{gt/gt}$ aortas. PRCP$^{gt/gt}$ aortas demonstrated decreased mRNA expression of the vascular transcription factors Kruppel-like-factor-2 (KLF2) and KLF4 and 2 of their downstream genes, eNOS and thrombomodulin ($P < .01$; Figure 5D).[27,28] In contrast, these mRNA were unchanged in PRCP$^{gt/gt}$ renal tissue (supplemental Figure 3). These findings suggested that vascular tissue ROS reduced expression of genes associated with anticoagulant function, which is associated with the shorter arterial thrombosis times of PRCP$^{gt/gt}$ mice.

Influence of PRCP on cellular ROS expression

We next determined whether cell PRCP levels themselves influenced ROS expression and loss of endothelial cell anticoagulation. PRCP knockdown in HUVEC by siRNA had 2.6% *PRCP* gene and 33% PRCP antigen expression, respectively (Figure 6A; supplemental Figure 4). PRCP siRNA-treated HUVECs demonstrated 2.1-fold increased constitutive DHE fluorescent intensity compared with control siRNA transfections ($P < .01$; Figure 6B). Similarly, MEFs from PRCP$^{gt/gt}$ mice, which expressed 0.4% PRCP mRNA compared with MEFs made from WT embryos, demonstrated 1.4-fold increased DHE fluorescence intensity compared with WT ($P = .048$; Figure 6C; supplemental Figure 4). PRCP-depleted HUVECs lost more than 90% of their ability to activate protein C ($P = .01$) without significant change in thrombomodulin antigen ($P = .30$), suggesting that thrombomodulin became dysfunctional (Figure 6D-E). In addition, PRCP depletion resulted in a 40% reduction in eNOS mRNA ($P = .02$) and increased uncoupled/coupled eNOS ratio ($P = .02$; Figure 6F-G). These combined data indicated that reduction of PRCP alone increased uncoupled eNOS and cell ROS and the increased cell ROS is associated with reduced protein C activation.
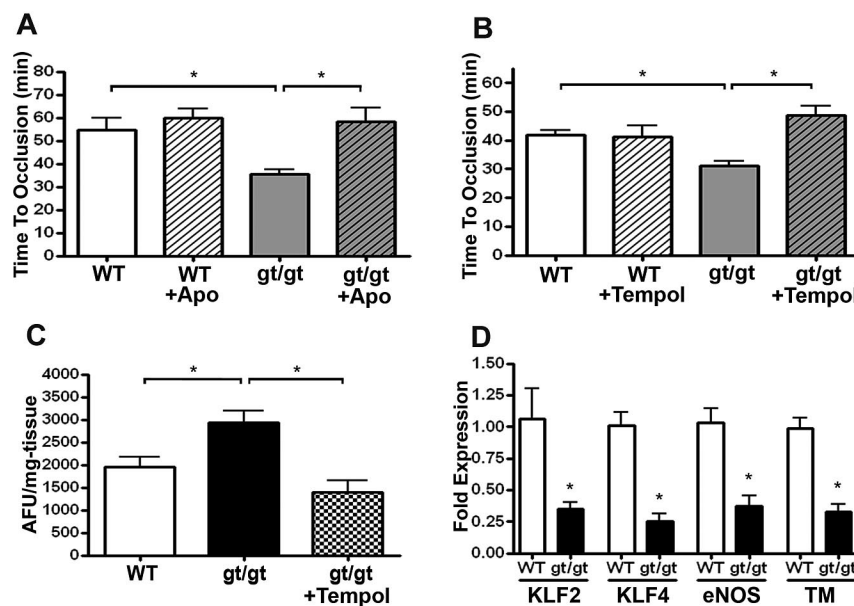

Figure 5. Influence of antioxidant therapy on time to arterial thrombosis occlusion. WT (n = 6) and PRCP$^{gt/gt}$ (n = 8) mice were left untreated or treated with the antioxidants apocynin (Apo; n = 6 WT; n = 11 PRCP$^{gt/gt}$; A) or tempol (n = 6 WT; n = 5 PRCP$^{gt/gt}$; B) for 7 days. At the conclusion of the treatment period, carotid artery occlusion times were performed using the Rose-Bengal carotid artery thrombosis model. One-way analysis of variance was used to determine the difference among groups. Data presented are the mean ± SEM of ≥ 5 mice for each condition. (C) Hydrogen peroxide (H$_2$O$_2$) levels were measured by Amplex Red in renal tissue harvested from WT (n = 7), PRCP$^{gt/gt}$ (n = 9), or PRCP$^{gt/gt}$ + tempol-treated (n = 5) mice. (D) Constitutive aortic expression of endothelial cell mRNA for KLF2, KLF4, eNOS, or thrombomodulin (TM) in WT (n = 3) or PRCP$^{gt/gt}$ (n = 4) mice. *$P < .05$.
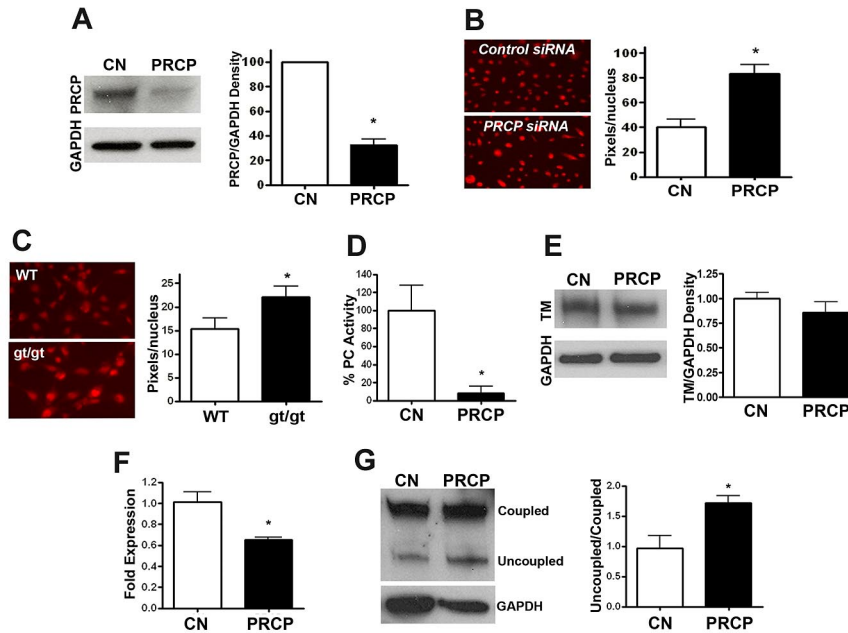
Figure 6. Influence of PRCP depletion in cultured cells. (A) HUVECs were treated with control (CN) or PRCP siRNA overnight, and comparative PRCP expression levels were analyzed by immunoblot. Data are mean ± SEM of 3 samples. (B) DHE fluorescent images of siRNA-treated HUVECs were obtained after control (CN; n = 6) or PRCP knockdowns (n = 6). Data are a representative experiment on siRNA-treated cells, and the adjacent graph is the mean ± SEM of pixel density per nucleus measured by morphometric analysis of 6 experiments for each group. (C) DHE fluorescent image of MEFs from control (n = 10) and PRCP$^{gt/gt}$ (n = 11) embryos. The figure presented is a representative experiment on each of the cells, and the adjacent graph is the mean ± SEM of pixel density per nucleus measured by morphometric analysis of ≥ 10 experiments for each condition. (B-C) Photographed at 40× on a Nikon, TE200 immunofluorescent microscope aperture 0.75/0.17 WD 0.72 oil immersion. The relative DHE fluorescence was measured by morphometric analysis on 40× microscopic images using MetaMorph (Molecular Devices). (D) Protein C activation on HUVECs with control (CN) or PRCP siRNA treatment as measured by activated protein C hydrolysis of a chromogenic substrate. Data presented are the percentage activated protein C hydrolysis generated on HUVECs treated with PRCP siRNA versus control. Data are mean ± SEM of 6 experiments per condition. (E) Thrombomodulin (TM) in HUVECs treated with control (CN) or PRCP siRNA as seen on immunoblot. Data presented are the mean ± SEM ratio of TM antigen/GAPDH antigen of 4 experiments. (F) mRNA expression for eNOS from control (CN) or PRCP knockdown siRNA-treated HUVECs as measured by real-time PCR (control: n = 7, PRCP knockdown: n = 7). (G) An immunoblot for eNOS was performed on control and PRCP siRNA-treated HUVEC lysates. The normalized relative ratio of uncoupled:coupled eNOS in lysates from 3 samples of control or PRCP siRNA-treated cells were compared by analysis of band intensity using densitometer scanning. Immunoblot of GAPDH was used as a loading control. *$P < .05$.

Discussion

These combined data demonstrate that PRCP deficiency is associated with higher blood pressure and shorter arterial thrombosis times. The PRCP$^{gt/gt}$ murine phenotype is dramatic considering that the animal is not a complete knockout and low levels of PRCP are expressed. This fact heightens the physiologic importance of PRCP. Other gene-trap mice have been characterized as hypomorphs rather than true knockouts.[29] Recent investigations indicate that the absence of hypothalamic PRCP results in reduced α-MSH$_{1-13}$ metabolism associated with animal leanness.[12] These data are consistent with the gene-wide study, suggesting that PRCP is a risk factor for the metabolic syndrome.[11] Furthermore, the finding that the mice are hypertensive is consistent with human studies showing that a polymorphism E112D in PRCP is associated with hypertension and preeclampsia.[8,9] Unlike other proteins related to the plasma kallikrein/kinin system (factor XII, high molecular weight kininogen, and the bradykinin B2 receptor), deficiency of PRCP is associated with a prothrombotic state rather than thrombosis protection.[16,30,31]

The finding that PRCP$^{gt/gt}$ are hypertensive and it is ameliorated by mitoTEMPO, an antioxidant directed to mitochondria, suggests that endothelial cell injury may be occurring because of increased ROS. We determined that there is a constitutive increase in uncoupled eNOS and tissue ROS in these animals. Our current understanding is that the ROS seen in the gene-trap tissue is directly related to the constitutive levels of PRCP. When HUVEC

PRCP is knocked down by siRNA, there is increased cell ROS. Further, murine embryonic fibroblasts made from the gene-trap embryos constitutively express higher ROS. In addition, the ROS expression is related to the prothrombotic phenotype of the PRCP$^{gt/gt}$ mice. When these mice are treated with 2 nonspecific antioxidants, apocynin or Tempol, the time to arterial thrombosis of the PRCP$^{gt/gt}$ mice lengthens to the normal control and the tissue ROS normalizes in the treated animals. These combined data indicate that both the higher blood pressure and arterial occlusion times in PRCP$^{gt/gt}$ mice are linked to vascular ROS.

The observed prothrombotic phenotype of PRCP hypomorphs is supported with pharmacologic studies with Z-Pro-Prolinal, a class prolyloligopeptidase inhibitor. Interestingly, using 2 murine backgrounds, inhibitors to plasma kallikrein also shortened the time to carotid artery thrombosis. Previous studies indicate that the use of PFRCK lengthened the time to arterial thrombosis in mice presumably because it inhibits factor XIIa.[30,32] These findings were surprising considering that PFRCK is a 23-fold better plasma kallikrein inhibitor than factor XIIa.[33] In our thrombosis assays, PFRCK shortens the time to carotid artery thrombosis in 2 mouse genetic backgrounds with different untreated times to arterial occlusion (∼ 50 minutes for C57BL/6 and ∼ 25 minutes for 129 svj). Similarly, SBTI, a 61-fold better inhibitor of plasma kallikrein than factor XIa, also shortened the time to thrombosis in both mouse strains. SBTI inhibits several blood coagulation enzymes, but in all cases but plasma kallikrein, one would expect lengthening of the time to thrombosis, not shortening. Confirmation that plasma kallikrein inhibition shortens arterial thrombosis
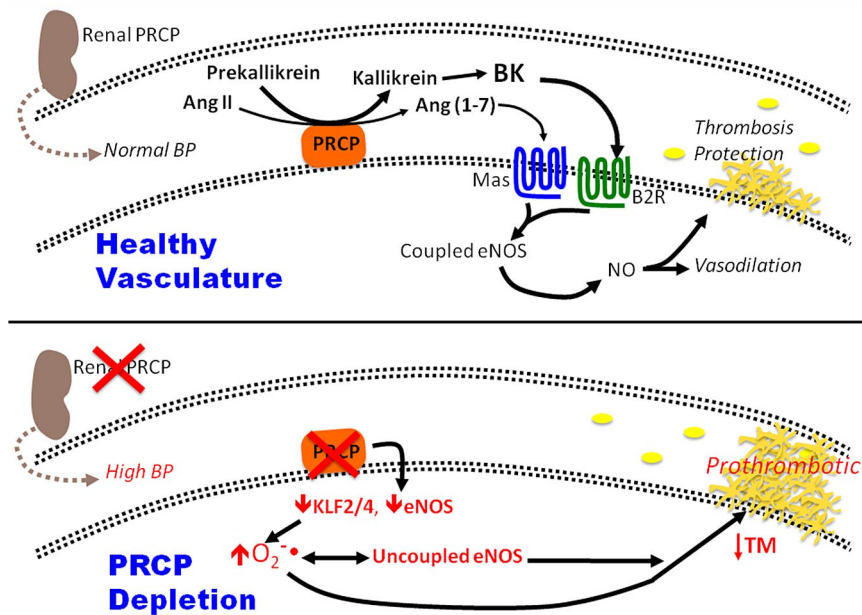
Figure 7. The influence of PRCP depletion in the intravascular compartment. (Top) At physiologic levels of PRCP, the enzyme contributes to the maintenance of normal blood pressure and reduces thrombosis risk in the intravascular compartment. PRCP activates prekallikrein to plasma kallikrein that then liberates bradykinin (BK) from kininogen. PRCP also degrades angiotensin II (Ang II) to angiotensin-(1-7) [Ang(1-7)].(4-6) Both BK and Ang (1-7) act on their respective endothelial cell membrane receptors, the bradykinin B2 receptor (B2R) or Mas, to increase coupled eNOS leading to NO formation, vasodilation, and thrombosis protection. (Bottom) PRCP-depleted mice are hypertensive with faster arterial thrombosis times. Reduction in aortic PRCP is associated increased tissue and cell ROS ($O_2{}^-$) and uncoupled eNOS. These findings are associated with reduced vascular KLF2, KLF4, eNOS, and thrombomodulin (TM).

times was performed by the use of the very specific inhibitor PKSI-527.[13] These data suggest that, unlike other plasma contact system proteins, inhibition of plasma kallikrein, like PRCP depletion or inhibition, increases arterial thrombosis risk. This observation is relevant to the developing clinical use of plasma kallikrein inhibitors to treat angioedema and reduce bleeding in cardiopulmonary bypass.

The mechanism(s) by which PRCP deficiency leads to arterial thrombosis was not obvious. Because PRCP activation of prekallikrein leads to bradykinin formation and PRCP degrades angiotensin II, we postulated that reduced bradykinin (BK) formation and higher angiotensin II levels would produce a prothrombotic state. However, plasma BK and angiotensin II levels were unchanged from control WT mice. Although plasma BK and angiotensin II levels were unchanged in PRCP[gt/gt], these data do not exclude decreased cell-surface production of these peptides contributing to their thrombosis and hypertension. Because normal plasma kininogen concentrations are approximately 2.5μM and plasma bradykinin concentrations are approximately 0.25nM, less than 0.01% of the total amount of the peptide is released into plasma. In addition, intracellular kallikrein/kinin and renin-angiotensin systems have been described, which also may be contributory to endothelial cell function in PRCP[gt/gt] mice.[34,35] The 60% normal plasma factor XII levels seen in the gene-trap mice are probably of no significance. Although epidemiologic studies suggest that reduced plasma factor XII levels are associated with myocardial infarction, mice severely deficient in factor XII are protected from thrombosis and plasma levels of factor XII of only 10% to 15% in humans are sufficient to have normal blood coagulation times.[30,36,37] Alternatively, in plasma from PRCP-deleted mice, there is a small but significant increase in contact activation-induced thrombin generation and a nonsignificant increase in tissue factor-induced thrombin generation. The exact mechanism for increased thrombin genera-

tion in plasma of PRCP[gt/gt] mice is not completely known, but it may be related to ROS and vascular dysfunction.

Vascular ROS in PRCP[gt/gt] mice is associated with endothelial cell dysfunction because the protective transcription factors KLF2 and KLF4 are reduced in the aorta. The anticoagulant genes thrombomodulin and eNOS, which are regulated by KLF2 and KLF4, are reduced in gene-trap mice aorta.[27,28,38] Further, siRNA knockdowns of PRCP in HUVECs are associated with increased uncoupled eNOS and markedly reduced protein C activation. The finding that thrombomodulin antigen in the knockdowns is not reduced indicates that it has become inactivated. ROS has been demonstrated to inactivate a critical methionine for thrombomodulin function.[39] How cellular and tissue ROS arise in PRCP-depleted states is not known. It is known that, when bradykinin binds the bradykinin B2 receptor, the latter is released from an inhibitory complex on eNOS.[40] It is possible that reduced cell surface or intracellular BK formation from less PRCP directly reduces cell eNOS activity contributing to increased ROS. In addition, reduced PRCP could result in less angiotensin II degradation, allowing for higher local levels. Angiotensin II is a potent stimulator of ROS formation through NADPH oxidase.[41]

In conclusion, these data suggest PRCP expression has a role in regulating blood pressure and arterial occlusion times. In normal animals, PRCP contributes to the production of bradykinin and angiotensin.[1-7] Both peptides bind to their constitutive receptors, the B2R and Mas, to contribute to the constitutive level of vascular NO that contributes to thrombosis protection (Figure 7). Alternatively, PRCP[gt/gt] mice are hypertensive. The reduction in PRCP in vivo results in reduced vascular KLF2/KLF4 and eNOS, contributing to increased vascular ROS and uncoupled eNOS (Figure 7). In addition, reduction in Kruppel-like factors contributes to reduced thrombomodulin, and the vascular ROS leads to its inactivation as well.[41] Both uncoupled eNOS and inactivated thrombomodulin

contribute to the increased arterial thrombosis risk seen in these animals. These combined data suggest that PRCP regulates blood pressure and arterial occlusion times, and both activities are linked to vascular ROS expression.

Acknowledgments

Authorship

Contribution: G.N.A., G.A.L., E.S., Y.Z., M.T.N., Y.C., Y.L., F.M., Z.S.-M., and L.G.D. performed research; Y.O. contributed a vital new reagent; G.H.J. analyzed and interpreted histologic data; and G.N.A., M.K.J., and A.H.S. designed research, analyzed and interpreted data, and wrote the manuscript.

Conflict-of-interest disclosure: The authors declare no competing financial interests.

Correspondence: Alvin H. Schmaier, Case Western Reserve University, 10900 Euclid Ave, WRB2-130, Cleveland, OH 44106-7284; e-mail: Schmaier@case.edu.

References

1. Abeywickrema PD, Patel SB, Byrne NJ, et al. Expression, purification and crystallization of human prolylcarboxypeptidase. *Acta Crystallogr Sect F Struct Biol Cryst Commun.* 2010;F66:702-705.

2. Soisson SM, Patel SB, Abeywickrema PD, et al. Structural definition and substrate specificity of the S28 protease family: the crystal structure of human prolylcarboxypeptidase. *BMC Struct Biol.* 2010;10(1):16.

3. Yang HY, Erdos EG. Second kininase in human blood plasma. *Nature.* 1967;215(5108):1402-1403.

4. Shariat-Madar Z, Mahdi F, Schmaier AH. Identification and characterization of prolylcarboxypeptidase as an endothelial cell prekallikrein activator. *J Biol Chem.* 2002;277(20):17962-17969.

5. Shariat-Madar Z, Mahdi F, Schmaier AH. Recombinant prolylcarboxypeptidase activates plasma prekallikrein. *Blood.* 2004;103(12):4554-4561.

6. Skidgel RA, Erdos EG. Cellular carboxypeptidases. *Immunol Rev.* 1998;161:129-141.

7. Javerzat S, Franco M, Herbert J, et al. Correlating global gene regulation to angiogenesis in the developing chick extra-embryonic vascular system. *PLoS One.* 2009;4(11):e7856.

8. Wang L, Feng Y, Zhang Y, et al. Prolylcarboxypeptidase gene, chronic hypertension, preeclampsia. *Am J Obstet Gynecol.* 2006;195(1):162-171.

9. Zhang Y, Hong XM, Xing HX, Li JP, Huo Y, Xu XP. E112D polymorphism in the prolylcarboxypeptidase gene is associated with blood pressure response to benazepril in Chinese hypertensive patients. *Chin Med J (Engl).* 2009;122(20):2461-2465.

10. Qin XP, Zheng SY, Tian HH, et al. Involvement of prolylcarboxypeptidase in the effect of rutaecarpine on the regression of mesenteric artery hypertrophy in renovascular hypertension rats. *Clin Exp Pharmacol Physiol.* 2009;36(3):319-324.

11. McCarthy JJ, Meyer J, Moliterno DJ, Newby LK, Rogers WJ, Topol EJ. GenQuest multicenter study: evidence for substantial effect modification by gender in a large-scale genetic association study of the metabolic syndrome among coronary heart disease patients. *Hum Genet.* 2003;114(1):87-98.

12. Wallingford N, Perroud B, Gao Q, et al. Prolylcarboxypeptidase regulates food intake by inactivating alpha-MSH in rodents. *J Clin Invest.* 2009(8);119:2291-2303.

13. Okada Y, Tsuda Y, Tada M, et al. Development of plasma kallikrein selective inhibitors. *Biopolymers.* 1999;51(1):41-50.

14. Skarnes WC, Moss JE, Hurtley SM, Beddington RSP. Capturing genes encoding membrane and secreted proteins important for mouse development. *Proc Natl Acad Sci U S A.* 1995;92(14):6592-6596.

15. Whitesall SE, Hoff JB, Vollmer AP, D'Alecy LG. Comparison of simultaneous measurement of mouse systolic arterial blood pressure by radiotelemetry and tail-cuff methods. *Am J Physiol Heart Circ Physiol.* 2004;286(6):H2408-H2415.

16. Shariat-Madar Z, Mahdi F, Warnock M, et al. Bradykinin B2 receptor knockout mice are protected from thrombosis by increased nitric oxide and prostacyclin. *Blood.* 2006;108(1):192-199.

17. Takimoto E, Champion HC, Li M, et al. Oxidant stress from nitric oxide synthase-3 uncoupling stimulates cardiac pathologic remodeling from chronic pressure load. *J Clin Invest.* 2005;115(5):1221-1231.

18. Schmaier AH, Zuckerberg A, Silverman C, Kuchibhotla J, Tuszynski GP, Colman RW. High molecular weight kininogen: a secreted platelet protein. *J Clin Invest.* 1983;71(5):1477-1489.

19. Hoffmann DS, Weydert CJ, Lazartigues E, et al. Chronic Tempol prevents hypertension, proteinuria, and poor feto-placental outcomes in BPH/5 mouse model of preeclampsia. *Hypertension.* 2008;51(4):1058-1065.

20. Guzik TJ, Channon KM. Measurement of vascular reactive oxygen species production by chemiluminescence. In: Fennell JP, Baker AH, eds. *Methods in Molecular Medicine, Vol. 108: Hypertension: Methods and Protocols.* Totowa NJ: Humana Press; 2005:73-89.

21. Ohishi N, Ohkawa H, Miike A, Tatano T, Yagi K. A new assay method for lipid peroxides using a methylene blue derivative. *Biochem Int.* 1985;10(2):205-211.

22. Samuelson LC, Metzger JM. Isolation and freezing of primary mouse embryonic fibroblasts (MEF) for feeder plates. *Cold Spring Harb Protoc*; 2006; doi: 10.1101/pdb.prot4482.

23. Haensly WE, Granger HJ, Morris AC, Cioffe C. Proximal-tubule-like epithelium in Bowman's capsule in spontaneously hypertensive rats. *Am J Pathol.* 1982;107(1):92-97.

24. Isaac J, Togel FE, Westenfelder C. Extent of glomerular tubularization is an indicator of the severity of experimental acute kidney injury in mice. *Nephron Exp Nephrol.* 2007;105(1):e33-e40.

25. Dikalova AE, Bikineyeva AT, Budyn K, et al. Therapeutic targeting of mitochondrial superoxide in hypertension. *Circ Res.* 2010;107(1):106-116.

26. Ferroni P, Basili S, Paoletti V, Davi G. Endothelial dysfunction and oxidative stress in arterial hypertension. *Nutr Metab Cardiovasc Dis.* 2006;16(3):222-233.

27. Hamik A, Lin Z, Kumar A, et al. Kruppel-like factor 4 regulates endothelial inflammation. *J Biol Chem.* 2007;282(18):13769-13779.

28. Atkins GB, Jain MK. Role of Kruppel-like transcription factors in endothelial biology. *Circ Res.* 2007;100(12):1686-1695.

29. Hyvarinen J, Hassinen IE, Sormunen R, et al. Hearts of hypoxia-inducible factor prolyl 4-hydroxylase-2 hypomorphic mice show protection against acute ischemia-reperfusion injury. *J Biol Chem.* 2010;285(18):13646-13657.

30. Renne T, Pozgajova M, Gruner S, et al. Defective thrombus formation in mice lacking coagulation factor XII. *J Exp Med.* 2005;202(2):271-281.

31. Merkulov S, Zhang WM, Komar AA, et al. Deletion of murine kininogen gene 1 (Kng1) causes loss of plasma kininogen and delays thrombosis. *Blood.* 2008;111(3):1274-1281.

32. Kannemeier C, Shibamiya A, Nakazawa F, et al. Extracellular RNA constitutes a natural procoagulant cofactor in blood coagulation. *Proc Natl Acad Sci U S A.* 2007;104(15):6388-6393.

33. Kettner C, Shaw E. Synthesis of peptides of arginine chloromethyl ketone: selective inactivation of human plasma kallikrein. *Biochemistry.* 1978;17(22):4778-4784.

34. Fink E, Bhoola KD, Snyman C, Neth P, Figueroa CD. Cellular expression of plasma prekallikrein in human tissues. *Biol Chem.* 2007;388(9):957-963.

35. Re R. Intracellular rennin-angiotensin system: the tip of the intracrine physiology iceberg. *Am J Physiol Heart Circ Physiol.* 2007;18(5):208-214.

36. Doggen CJ, Rosendaal FR, Meijers JC. Levels of intrinsic coagulation factors and the risk of myocardial infarction among men: opposite and synergistic effects of factors XI and XII. *Blood.* 2006;108(13):4045-4051.

37. Meier HL, Pierce JV, Colman RW, Kaplan AP. Activation and function of human Hageman factor: the role of high molecular weight kininogen and prekallikrein. *J Clin Invest.* 1977;60(1):18-31.

38. Lin Z, Kumar A, SenBanerjee S, et al. Kruppel-like Factor 2 (KLF2) regulates endothelial thrombotic function. *Circ Res.* 2005;96(5):e48-e57.

39. Glaser CB, Morser J, Clarke JH, et al. Oxidation of a specific methionine in thrombomodulin by activates neutrophil products blocks cofactor activity. *J Clin Invest.* 1992;90(6):2565-2573.

40. Golser R, Gorren AC, Leber A, et al. Interaction of endothelial and neuronal nitric-oxide synthases with the bradykinin B2 receptor: binding of an inhibitory peptide to the oxygenase domain blocks uncoupled NADPH oxidation. *J Biol Chem.* 2000;275(8):5291-5296.

41. Wingler K, Wunsch S, Kreutz R, Rothermund L, Paul M, Schmidt HH. Up-regulation of the vascular NAD(P)H-oxidase isoforms Nox1 and Nox4 by the renin-angiotensin system in vitro and in vivo. *Free Radic Biol Med.* 2001;31(11):1456-1464.